Journal of Solid State Chemistry **160,** 178–183 (2001)
doi:10.1006/jssc.2001.9217, available online at http://www.idealibrary.com on IDEAL®

Single Crystal Growth and Structural Chemistry of $Li_{1-z}Ni_{1+z}O_2$ with $z = 0.075$

Yasuhiko Takahashi, Junji Akimoto,[1] Yoshito Gotoh, Kenji Kawaguchi, and Susumu Mizuta

National Institute of Advanced Industrial Science and Technology,[2] 1-1-1 Higashi, Tsukuba, 305-8565, Japan

Received November 2, 2000; in revised form April 11, 2001; accepted April 20, 2001

Single crystals of the lithium nickel dioxide compound $Li_{1-z}Ni_{1+z}O_2$ with $z = 0.075$ have been successfully synthesized by a flux method for the first time. A single-crystal X-ray diffraction study confirmed trigonal symmetry, $R\bar{3}m$ space group, and the lattice parameters $a = 2.8899(13)$ Å and $c = 14.1938(17)$ Å. The cation distribution in $Li_{0.925}Ni_{1.075}O_2$ was determined to be $(Li_{0.744}Ni_{0.256})_{3a}[Li_{0.181}Ni_{0.819}]_{3b}O_2$ with a final R value of 2.68% using 202 independent observed reflections. The relationships between cation distributions and structural parameters for $Li_{1-z}Ni_{1+z}O_2$ compounds have been summarized and discussed using the 37 reported structural data. The magnetization measurements of the present single crystal samples confirmed the history dependence of temperature versus M/H maximum at about 60 K. © 2001 Academic Press

Key Words: **lithium battery; crystal growth; two-dimensional triangular lattice; single-crystal X-ray structure analysis.**

INTRODUCTION

Lithium nickel dioxide with the α-$NaFeO_2$ structure, $LiNiO_2$, was reported for the first time by Dyer *et al.* (1). This material can be considered as the end member ($z = 0$) of the $Li_{1-z}Ni_{1+z}O_2$ solid solution system (2, 3). In the ideal crystal structure of $LiNiO_2$ with $R\bar{3}m$ space group, alternate layers of lithium and nickel occupy the octahedral voids of a cubic close-packed (ccp) oxygen arrangement making up the two-dimensional triangular lattice, as illustrated in Fig. 1. It is well established that the stoichiometric $LiNiO_2$ compound is very difficult to obtain, because the high-temperature treatment of $LiNiO_2$ leads to decomposition from $LiNiO_2$ to $Li_{1-z}Ni_{1+z}O_2$ solid solution compounds with the partially disordered α-$NaFeO_2$ structure (4).

Since Hirakawa *et al.* (5) first pointed out that $LiNiO_2$ is suitable as a model of an $S = \frac{1}{2}$ antiferromagnetic triangular lattice with an Ising-like anisotropy, a wide variety of magnetic behaviors have been reported for $LiNiO_2$ and the solid solution $Li_{1-z}Ni_{1+z}O_2$ ($0 < z < 1$) with different chemical compositions and cation distributions (6–8). Recently, the solid state chemistry of $Li_{1-z}Ni_{1+z}O_2$ has been intensively investigated, since this compound and its derivatives are used as the positive electrode materials in low-cost and high-energy-density rechargeable lithium batteries (4, 9–12). Battery capacity is very sensitive to any departure from the ideal $LiNiO_2$ stoichiometry, so numerous studies have been devoted to understand the relationship between various synthetic conditions and nonstoichiometry in $Li_{1-z}Ni_{1+z}O_2$ (13–15). Using these well-characterized powder samples, the intrinsic magnetic properties have been clarified for $Li_{1-z}Ni_{1+z}O_2$ (16–20), and for $LiNiO_2$ as a physical realization of a quantum spin–orbital liquid (21–23).

Single crystal specimens are needed to clarify the precise crystal structure and intrinsic physical property of $LiNiO_2$ and $Li_{1-z}Ni_{1+z}O_2$, but such single crystals have not yet been synthesized. In the present study, we report single crystal synthesis and X-ray structure refinement of the first single crystal of $Li_{1-z}Ni_{1+z}O_2$. We will also summarize the relationships between the cation distributions and the structural parameters for the $Li_{1-z}Ni_{1+z}O_2$ compounds using the 37 reported structural data.

EXPERIMENTAL

Single crystals were grown by a flux growth method using a vertical resistance furnace. The as-prepared $LiNiO_2$ powder (Nippon Chemical Industrial Co., Ltd., Japan) was mixed with Li_2O_2 (99.9%) and LiCl (99.9%) to form flux material in the nominal weight ratio of $LiNiO_2$:Li_2O_2:LiCl = 1:4:4. The mixture was heated to 1173 K for 10 h in a gold crucible, gradually cooled to 873 K at a rate of 3 K/h, and then cooled naturally. The eutectic melting point of the optimal flux composition was estimated to be about 780 K. The products were easily separated from the frozen Li–O–Cl system flux in air because of the deliquescence of the flux material. Black, triangular platelet single crystals of

[1] To whom correspondence should be addressed. E-mail: j.akimoto@aist.go.jp. Fax: + 81-298-61-4555.

[2] Formerly, the National Institute of Materials and Chemical Research.

0022-4596/01 $35.00

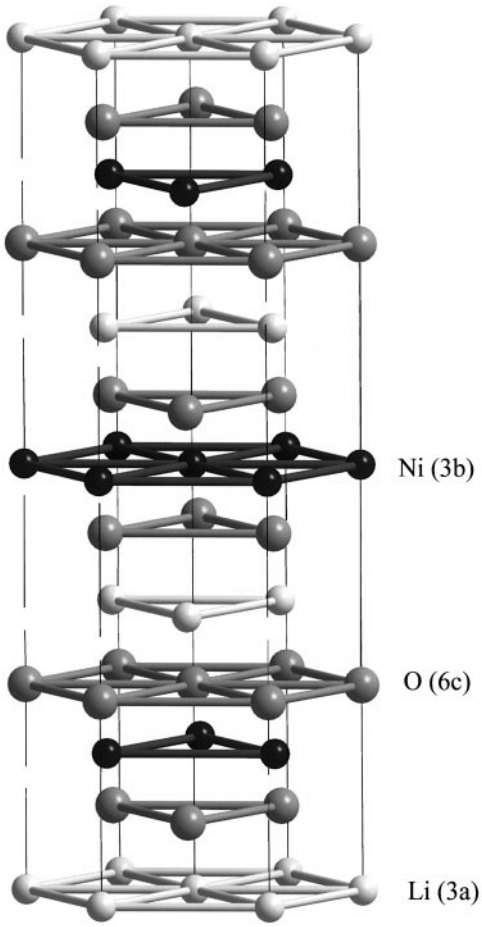

FIG. 1. Ideal ordered rocksalt structure of $LiNiO_2$, drawn with DIAMOND (27).

about $0.5 \times 0.5 \times 0.2\,mm^3$ at maximum were obtained, as shown in Fig. 2.

Chemical analyses of selected single crystals were carried out by using SEM-EDX (JEOL JSM-5400) and inductively coupled plasma (ICP) spectroscopy. EDX analysis showed that the crystals were free from gold contamination from the crucible. The chemical formula, analyzed by ICP using the pulverized sample (about 30 mg), was $Li_{0.9}Ni_{1.1}O_2$, which is consistent with the result of the present structure refinement.

Three single crystal specimens were carefully examined with an X-ray precession camera (Mo$K\alpha$ radiation) in order to check on crystal quality and to determine the lattice parameters, systematic extinctions, and possible superstructures. We could not find any superstructures, and successfully indexed to the trigonal lattice, space group $R\bar{3}m$. The determined lattice parameters for three specimens were in good agreement with each other within the experimental error. This fact suggested the chemical homogeneity of the single crystal products under the present crystal growth conditions.

A small crystal, $0.03 \times 0.03 \times 0.02\,mm^3$ in size, was used for the intensity data collection. A summary of experimental and crystallographic data is given in Table 1. The intensity data were collected in the 2θ–ω scan mode at a scan rate of 1.0°/min at 300 K on the four-circle diffractometer (operating conditions: 50 kV, 250 mA) using graphite-monochromatized Mo$K\alpha$ radiation ($\lambda = 0.71073$ Å). A total of 1778 reflections were measured within the limit of $2\theta < 110^\circ$, and the averaged 202 independent reflections ($R_{int} = 6.23\%$) were used for structure refinement. Absorption and extinction corrections were performed. All calculations were carried out using the *Xtal3.7* program (24).

In the structure analysis that followed, we adopted the space group of highest symmetry, $R\bar{3}m$, which had been confirmed by successful refinement. The refinement was initiated with the atomic coordinates of Li at the 3*a* $(0, 0, 0)$ site, Ni at the 3*b* $(0, 0, \frac{1}{2})$ site, and O at the 6*c* $(0, 0, z)$ site. Further site population refinements were applied using the three structural models shown in Table 2. These results clearly indicate that the Li and Ni atoms are located in both of the 3*a* and 3*b* sites, and the cation distribution in the present single crystal is $(Li_{0.744}Ni_{0.256})_{3a}[Li_{0.181}Ni_{0.819}]_{3b}O_2$. A difference Fourier synthesis, using the final atomic parameters, showed no significant residual peak. Finally, the structure was refined to $R = 2.68\%$ and w$R = 2.04\%$ for 202 reflections, with a shift/error for all 11 parameters of less than 0.001.

The temperature dependence of the magnetization of the present single crystals was measured using a SQUID magnetometer (Quantum Design) in a temperature range from 4.5 K to 300 K at applied fields of 20 and 100 Oe.

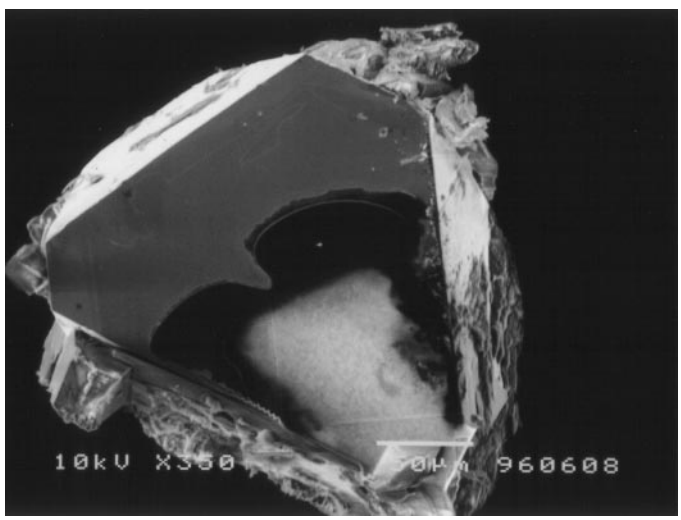

FIG. 2. SEM photograph of an $Li_{0.925}Ni_{1.075}O_2$ single crystal.

TABLE 1
Summary of Experimental and Crystallographic Data

Chemical formula	$Li_{0.925}Ni_{1.075}O_2$
Temperature (K)	300
Wavelength (Å)	0.71073
Crystal system	Trigonal
Space group	$R\bar{3}m$
Lattice parameters	
a (Å)	2.8899(13)
c (Å)	14.1938(17)
V (Å^3)	102.66(9)
Z	3
D_x (g/cm^3)	4.913
Crystal size (mm)	$0.03 \times 0.03 \times 0.02$
Maximum 2θ (°)	110
Absorption correction	Gaussian integration
Transmission factors	
Min.	0.676
Max.	0.845
Measured reflections	1778
Independent reflections	202 ($R_{int} = 6.23\%$)
Number of variables	11
Final goodness of fit	1.605
Final residuals	$R = 2.68\%$
	w$R = 2.04\%$ [$w = 1/\sigma^2 F$]
Extinction parameter g	$0.0037(12) \times 10^4$
Largest difference Fourier peak and hole (e/Å^3)	1.55 and -4.33

RESULTS AND DISCUSSION

Crystal Structure

A summary of the fundamental crystallographic data is given in Table 1. Final structural parameters and selected bond distances and angles are given in Tables 3 and 4, respectively.

The structure refinement revealed that the chemical composition of the present single crystal was $Li_{0.925}Ni_{1.075}O_2$, which corresponded to $Li_{1-z}Ni_{1+z}O_2$ with $z = 0.075$. The cation distribution in the present $Li_{0.925}Ni_{1.075}O_2$ was determined to be $(Li_{0.744}Ni_{0.256})_{3a}[Li_{0.181}Ni_{0.819}]_{3b}O_2$. The refined oxygen coordination parameter is $z(O) = 0.24420(10)$, which is slightly shifted from 0.24111(16) in the $Li_{0.996}Ni_{1.008}O_2$ polycrystalline sample (4) to the ideal oxygen packing value of 0.25. This fact is explained by the partial disordering of the cation distribution between the 3*a* and the 3*b* sites in $Li_{1-z}Ni_{1+z}O_2$. Indeed, the difference in the metal–oxygen M_{3a}–O (2.0939(11) Å) and M_{3b}–O (1.9987(9) Å) bond distances is smaller than those in more stoichiometric compounds, e.g., in $Li_{0.996}Ni_{1.008}O_2$ (4) (M_{3a}–O, 2.1154(14) Å; M_{3b}–O, 1.9692(12) Å). The lattice parameters and the cation distribution in the present $Li_{0.925}Ni_{1.075}O_2$ are highly consistent with those in the $Li_{0.9}Ni_{1.1}O_2$ powder sample (lattice parameters: $a = 2.8874$ Å, $c = 14.2214$ Å; structural formula $(Li_{0.87}Ni_{0.13})_{3a}[Li_{0.03}Ni_{0.97}]_{3b}O_2$) reported by Gummow and Thackeray (25).

TABLE 2
Three Structure Refinement Models and Their *R* Values

Model	Refined cation distribution	Composition	R	wR
I	$(Li_{0.760}Ni_{0.240})_{3a}[Li_{0.240}Ni_{0.760}]_{3b}O_2$	$LiNiO_2$	3.32	2.23
II	$(Li_{0.744}Ni_{0.256})_{3a}[Li_{0.181}Ni_{0.819}]_{3b}O_2$	$Li_{0.925}Ni_{1.075}O_2$	2.68	2.04
III	$(Li_{0.692}Ni_{0.308})_{3a}[Ni]_{3b}O_2$	$Li_{0.692}Ni_{1.308}O_2$	4.28	3.29

TABLE 3
Atomic Coordinates, Equivalent Isotropic Displacement Parameter U_{eq}, and Site Occupancy Factor g for $Li_{0.925}Ni_{1.075}O_2$

Atom	Position	x	y	z	U_{eq}	g
Li1	3*a*	0	0	0	0.0072(2)	0.744(4)
Ni1	3*a*	0	0	0	$=U_{eq}$(Li1)	$=1-g$(Li1)
Li2	3*b*	0	0	$\frac{1}{2}$	0.00556(9)	0.181(10)
Ni2	3*b*	0	0	$\frac{1}{2}$	$=U_{eq}$(Li2)	$=1-g$(Li2)
O	6*c*	0	0	0.24420(10)	0.0157(4)	1

Relationships between Cation Distributions and Structural Parameters

There are presently many structural reports for the non-stoichiometric $Li_{1-z}Ni_{1+z}O_2$ compounds. Most of them consider only additional Ni atoms at the 3*a* site, as shown in Fig. 3b. The corresponding structural formula is expressed as $(Li_{1-x}Ni_x)_{3a}[Ni]_{3b}O_2$ ($z = x$). However, some reports (25, 26) suggest the cation substitution for both the 3*a* and 3*b* sites with the structural formula $(Li_{1-x}Ni_x)_{3a}[Li_yNi_{1-y}]_{3b}O_2$ ($z = x - y$) (Fig. 3c), such as in the case of the present structure analysis. To clarify the relationships between cation distributions and structural parameters, we have summarized the 37 structural data, reported by Pickering *et al.* (26), Gummow and Thackeray (25), Reimers *et al.* (13), Kanno *et al.* (4), Hirano *et al.* (14), Rougier *et al.* (15), and the present single crystal study.

TABLE 4
Selected Bond Distances (Å) and Angles (°)

	M_{3a}–O Octahedron		
(Li, Ni)–O	2.0939(11)	O–(Li, Ni)–O	87.27(4)
O–O	2.8899(13)	O–(Li, Ni)–O′	92.73(4)
O–O′	3.0308(18)		
	M_{3b}–O Octahedron		
(Li, Ni)–O	1.9987(9)	O–(Li, Ni)–O	92.59(4)
O–O	2.8899(13)	O–(Li, Ni)–O′	87.41(4)
O–O′	2.7620(17)		

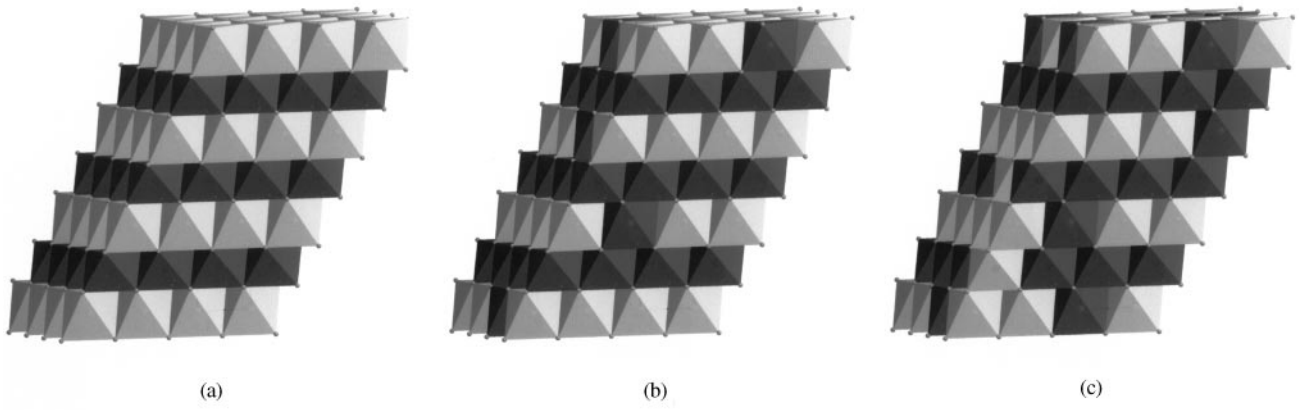

FIG. 3. Three cation distribution models for $Li_{1-z}Ni_{1+z}O_2$ compounds: (a) ideal $(Li)_{3a}[Ni]_{3b}O_2$ ($z = 0$), (b) $(Li_{1-x}Ni_x)_{3a}[Ni]_{3b}O_2$ ($z = x$), and (c) $(Li_{1-x}Ni_x)_{3a}[Li_yNi_{1-y}]_{3b}O_2$ ($z = x - y$). The black and gray octahedra correspond to NiO_6 and LiO_6, respectively.

Figure 4 shows the relationship between the axial ratio c/a and the z(O) parameter for oxygen atoms. As can be seen from this figure, we can classify these data in two main structural groups. One group (structure I) has the structural formula $(Li_{1-x}Ni_x)_{3a}[Ni]_{3b}O_2$, which means that some of the Li atoms at the 3*a* site are replaced by Ni atoms and only Ni atoms occupy the 3*b* site (Fig. 3b). The other group (structure II) has the disordered structural formula $(Li_{1-x}Ni_x)_{3a}[Li_yNi_{1-y}]_{3b}O_2$, which means that both the 3*a* and 3*b* sites are occupied by Li and Ni atoms (Fig. 3c). These structure groups can be divided by the c/a value of 4.915, as shown in Fig. 4.

Figure 5 shows a relationship between the c/a ratio and Ni occupancy at the 3*a* site. The c/a values decrease linearly together with increasing Ni content at the 3*a* site, toward the value of $2\sqrt{6}$ for ideal cubic closest packing. This figure indicates that the lithium replacement at the 3*b* site takes place only in the substitutional range of $x > 0.25$ in $(Li_{1-x}Ni_x)_{3a}[Li_yNi_{1-y}]_{3b}O_2$.

A relationship between the z(O) parameter for oxygen atoms and Li occupancy at the 3*b* site is shown in Fig. 6. The lithium replacement at the 3*b* site suddenly starts from $z(O) = 0.243$ and rapidly progresses. The present single-crystal structural data has the replacement value of $y = 0.181$ in $(Li_{1-x}Ni_x)_{3a}[Li_yNi_{1-y}]_{3b}O_2$. From these structural considerations, we can roughly estimate the structural parameters, i.e., z(O) parameter for oxygen atoms (Fig. 4), and site population parameters x and y in $(Li_{1-x}Ni_x)_{3a}[Li_yNi_{1-y}]_{3b}O_2$ (Figs. 5 and 6), using the c/a value of the lithium nickel dioxide $Li_{1-z}Ni_{1+z}O_2$ compounds.

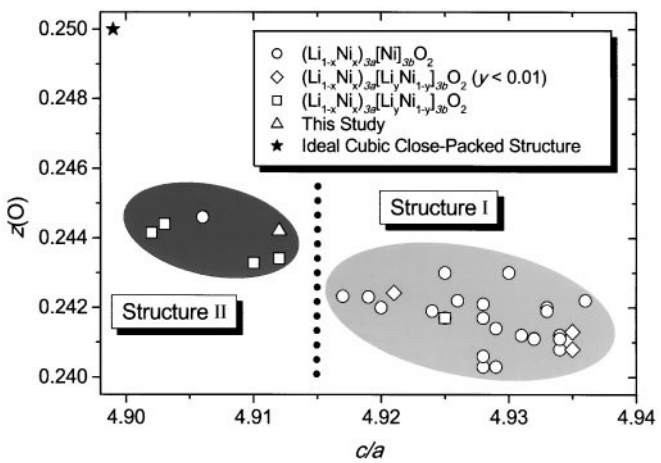

FIG. 4. Relationship between the axial ratio c/a and the z-parameter for oxygen atoms using the 37 reported structural data for $Li_{1-z}Ni_{1+z}O_2$.

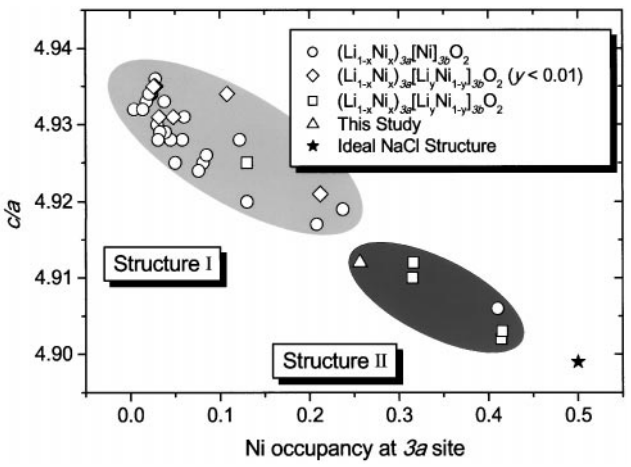

FIG. 5. Relationship between the axial ratio c/a and the Ni occupancy at the 3*a* site.

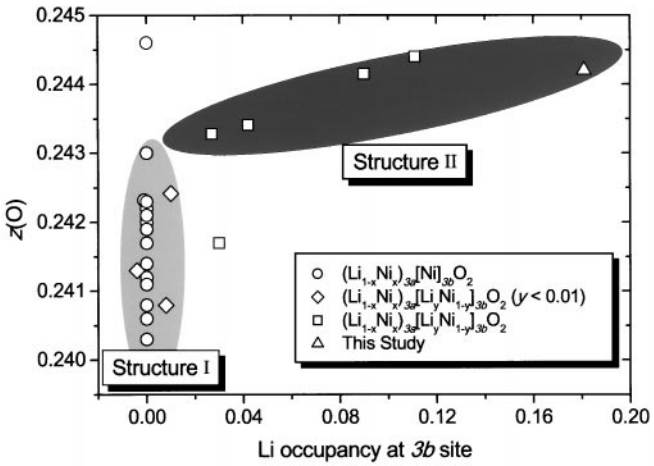

FIG. 6. Relationship between the z-parameter for oxygen atoms and the Li occupancy at the 3*b* site.

Magnetic Property

Magnetization (M) was measured as a function of temperature at fixed fields using the present $Li_{0.925}Ni_{1.075}O_2$ single crystal samples. Figure 7 shows a typical temperature dependence from 4.5 K to 300 K at 20 Oe. The open and filled marks correspond to measurements on field cooling and measurements on heating after zero-field cooling, respectively. The history dependence of temperature versus M/H maximum at about 60 K was clearly observed. Similar features were observed previously in the polycrystalline samples of $Li_{1-z}Ni_{1+z}O_2$ with $z = 0.12$ (16, 17) and $z = 0.08$ (20, 21). The predicted chemical composition based on the magnetization measurements was consistent with the result gained with the present structure refinement of $Li_{1-z}Ni_{1+z}O_2$ with $z = 0.075$.

It should be noted that the history dependence of a deviation from the Curie–Weiss law can be clearly seen between 150 K and 220 K at 20 Oe in Fig. 7, while the measurement at $H = 100$ Oe does not show any hysteresis above 120 K. Further precise magnetic properties of the present single crystal samples are now being examined.

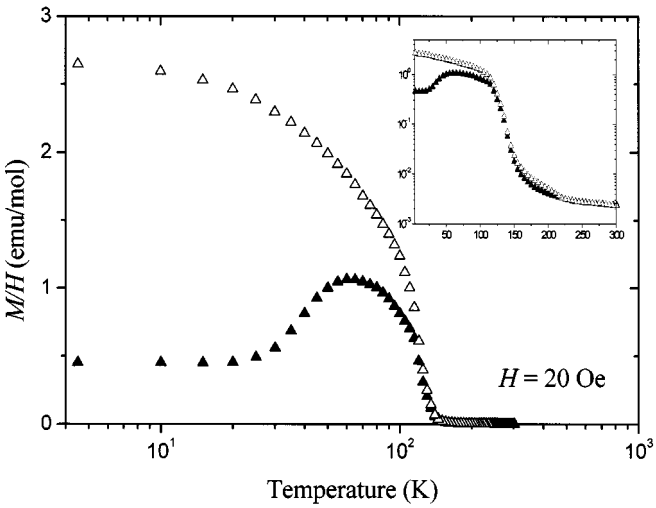

FIG. 7. Temperature dependence of the magnetization for $Li_{0.925}Ni_{1.075}O_2$ single crystals measured at $H = 20$ Oe after zero-field cooling (filled) and on-field cooling (open), respectively. The inset is a restyling with a linear temperature scale and a logarithmic M/H scale.

CONCLUSION

We have succeeded for the first time in growing single crystals of the lithium nickel dioxide $Li_{1-z}Ni_{1+z}O_2$ with $z = 0.075$. The structure refinement by the single-crystal X-ray diffraction method revealed the cation distribution in the present compound of $(Li_{0.744}Ni_{0.256})_{3a}[Li_{0.181}Ni_{0.819}]_{3b}O_2$. In order to clarify the intrinsic magnetism in $LiNiO_2$, it is important to synthesize more stoichiometric single crystal samples. However, it is very difficult to obtain the "perfectly stoichiometric $LiNiO_2$," even in the case of the powder samples (4), where the ordering of lithium and nickel atoms into alternate (111) planes of the cubic close-packed oxygen arrangement is essentially perfect (Fig. 1). A key in the synthesis of more stoichiometric single crystals is lowering the synthetic temperatures. A further study of single crystal synthesis by a modified flux method is now in progress.

REFERENCES

1. L. D. Dyer, B. S. Borie, and G. P. Smith, *J. Am. Chem. Soc.* **76,** 1499 (1954).
2. J. B. Goodenough, D. G. Wickham, and W. J. Croft, *J. Phys. Chem. Solids* **5,** 107 (1958).
3. V. W. Bronger, H. Bade, and W. Klemm, *Z. Anorg. Allg. Chem.* **333,** 188 (1964).
4. R. Kanno, H. Kubo, Y. Kawamoto, T. Kamiyama, F. Izumi, Y. Takeda, and M. Takano, *J. Solid State Chem.* **110,** 216 (1994).
5. K. Hirakawa, H. Kadowaki, and K. Ubukoshi, *J. Phys. Soc. Jpn.* **54,** 3526 (1985).
6. J. Akimoto and H. Takei, *J. Solid State Chem.* **85,** 31 (1990).
7. J. P. Kemp, P. A. Cox, and J. W. Hodby, *J. Phys.: Condens. Matter* **2,** 6699 (1990).
8. K. Hirota, Y. Nakazawa, and M. Ishikawa, *J. Phys.: Condens. Matter* **3,** 4721 (1991).
9. M. G. S. R. Thomas, W. I. F. David, J. B. Goodenough, and P. Groves, *Mater. Res. Bull.* **20,** 1137 (1985).
10. J. R. Dahn, U. von Sacken, and C. A. Michal, *Solid State Ionics* **44,** 87 (1990).
11. J. R. Dahn, U. von Sacken, M. W. Juzkow, and H. Al-Janaby, *J. Electrochem. Soc.* **138,** 2207 (1991).
12. C. Delmas, M. Ménétrier, L. Croguennec, S. Levasseur, J. P. Pérès, C. Puillerie, G. Prado, L. Fournès, and F. Weill, *Int. J. Inorg. Mater.* **1,** 11 (1999).
13. J. N. Reimers, J. R. Dahn, J. E. Greedan, C. V. Stager, G. Liu, I. Davidson, and U. von Sacken, *J. Solid State Chem.* **102,** 542 (1993).

14. A. Hirano, R. Kanno, Y. Kawamoto, Y. Takeda, K. Yamaura, M. Takano, K. Ohyama, M. Ohashi, and Y. Yamaguchi, *Solid State Ionics* **78,** 123 (1995).
15. A. Rougier, P. Gravereau, and C. Delmas, *J. Electrochem. Soc.* **143,** 1168 (1996).
16. A. Rougier, C. Delmas, and G. Chouteau, *J. Phys. Chem. Solids* **57,** 1101 (1996).
17. A.-L. Barra, G. Chouteau, A. Stepanov, A. Rougier, and C. Delmas, *Eur. Phys. J. B* **7,** 551 (1999).
18. F. Reynaud, A. M. Ghorayeb, Y. Ksari, N. Menguy, A. Stepanov, and C. Delmas, *Eur. Phys. J. B* **14,** 83 (2000).
19. M. D. Núñez-Regueiro, E. Chappel, G. Chouteau, and C. Delmas, *Eur. Phys. J. B* **16,** 37 (2000).
20. D. Mertz, Y. Ksari, F. Celestini, J. M. Debierre, A. Stepanov, and C. Delmas, *Phys. Rev. B* **61,** 1240 (2000).
21. K. Yamaura, M. Takano, A. Hirano, and R. Kanno, *J. Solid State Chem.* **127,** 109 (1996).
22. Y. Kitaoka, T. Kobayashi, A. Kôda, H. Wakabayashi, Y. Niino, H. Yamakage, S. Taguchi, K. Amaya, K. Yamaura, M. Takano, A. Hirano, and R. Kanno, *J. Phys. Soc. Jpn.* **67,** 3703 (1998).
23. Y. Q. Li, M. Ma, D. N. Shi, and F. C. Zhang, *Phys. Rev. Lett.* **81,** 3527 (1998).
24. S. R. Hall, D. J. du Boulay, and R. Olthof-Hazekamp, Eds. "Xtal3.7 System," University of Western Australia, Australia, 2000.
25. R. J. Gummow and M. M. Thackeray, *Solid State Ionics* **53–56,** 681 (1992).
26. I. J. Pickering, J. T. Lewandowski, A. J. Jacobson, and J. A. Goldstone, *Solid State Ionics* **53–56,** 405 (1992).
27. "DIAMOND: Visual Crystal Structure Information System," version 2.1, CRYSTAL IMPACT, Postfach 1251, D-53002 Bonn, Germany, 1999.